NJC

ROYAL SOCIETY OF CHEMISTRY

COMMUNICATION

View Article Online
View Journal | View Issue

Check for updates

Cite this: *New J. Chem.*, 2024, **48**, 6064

Received 30th January 2024,
Accepted 9th March 2024

DOI: 10.1039/d4nj00508b

rsc.li/njc

Capacitive CO_2 sensor made of aminated cellulose nanofibrils: development and optimization†

Frédéric Héraly, Anirban Sikdar, Jian Chang and Jiayin Yuan *

CO_2 sensors are very important; however, their performance is limited by stability and selectivity. This study unveils a capacitive CO_2 sensor with a dielectric layer comprised of amine-functionalized cellulose nanofibril (CNF) foam, significantly enhanced by the addition of 1,8-diazabicyclo[5.4.0]undec-7-ene (DBU). The core innovation of this research lies in the strategic use of CNF-based foam, which leads to a substantial increase in sensor capacitance, setting a new standard in CO_2 monitoring technologies. The sensor showcases exceptional performance under ambient conditions, with marked improvements in sensitivity towards CO_2. The advancements are attributed to the chemisorption properties of the aminated CNFs combined with the DBU enhancement, facilitating more effective CO_2 capture. By integrating these materials, we present a sensor that opens new avenues for environmental monitoring, healthcare diagnostics, and industrial safety, establishing a new benchmark for capacitive CO_2 sensors in efficiency and environmental sustainability.

Introduction

Our world is confronting an environmental challenge, accentuated by the escalating level of CO_2 concentration in the atmosphere.[1] As a crucial type of greenhouse gases,[2] CO_2 plays a pivotal role in driving climate change.[3] This alarming situation necessitates the need of efficient, sensitive, and selective CO_2 sensing technologies.[4–6] Such sensors are essential in applications ranging from environmental monitoring,[7] to healthcare diagnostics.[8]

The current CO_2 sensor technologies,[9] such as metal oxide semiconductors,[10] non-dispersive infrared,[11,12] and electrochemical ones, and recent works,[13,14] have made notable advancements. However, they often face limitations in terms of sensitivity, selectivity, and/or vulnerability to environmental variables like humidity, as well as issues of long-term stability.[15] These challenges underscore the urgency for innovative developments in CO_2 sensing materials and design concepts.[16]

To address these limitations, this research introduces a groundbreaking capacitive CO_2 sensor,[17,18] primarily based on chemical sensing principles, and employs aminated cellulose nanofibrils (CNFs) foams as the core sensing component. Indeed, in recent years, CNFs have emerged as a highly versatile material for a broad spectrum of sensing applications, as evidenced by their increasing presence in the literature.[19,20] They are also distinguished by their exceptional characteristics, such as high surface area, renewable nature, and biodegradability.[21–23]

Experimental section

Materials

TEMPO-oxidized cellulose nanofibrils (CNFs) were obtained from Nippon Paper Industries (Tokyo, Japan). 3-Aminopropyldiethoxymethylsilane (APDEMS) (97%), 1,8-diazabicyclo[5.4.0]undec-7-ene (98%), glycerol (≥99%), and Sun Tropic conductive graphite ink were obtained from Sigma-Aldrich. Aluminum foil (280 mm × 120 m × 15 μm) was obtained from VWR. High-purity CO_2 gas (>99.9%) was provided by Strandmöllen AB. A capacitance meter was acquired from RS Sweden. All materials were used as received.

Synthesis and processing

Fabrication of the FD-APDEMS-CNFs. The FD-APDEMS-CNFs hydrogel was prepared from a 0.75 wt% aqueous dispersion of CNFs with the subsequent addition of an APDEMS solution in a 5 : 1 mass ratio. After stirring the APDEMS-CNFs mixture at 300 rpm for 24 hours, the mixture was freeze-dried for at least 48 hours to obtain the final product. The rheological analysis of FD-APDEMS-CNFs, as illustrated in Fig. S1 (ESI†), reveals a constant storage modulus (G') of 3 Pa and a constant loss modulus (G'') of 1 Pa, indicating a predominance of elastic behavior over viscous properties.

Department of Materials and Environmental Chemistry, Stockholm University, Svante Arrheniusväg 16C, Stockholm 106 91, Sweden.
E-mail: Jiayin.Yuan@mmk.su.se

† Electronic supplementary information (ESI) available. See DOI: https://doi.org/10.1039/d4nj00508b

Fabrication of the capacitive CO_2 sensor

Dielectric layer formation. In the preparation of the dielectric layer, glycerol was added to the APDEMS-CNFs mixture to enhance its flexibility. This addition was in a 1 : 1 dry weight ratio, and the mixture was stirred vigorously for 1 minute to ensure homogeneity. Subsequently, 6 g of this mixture were transferred to a polypropylene beaker of 5.5 cm in diameter and 7.0 cm in height. The content in the beaker was then freeze-dried for 3 days. Following the freeze-drying process, the resultant foam was compressed under a 2 kg load for 30 seconds. This treatment resulted in the formation of the final dielectric layer, designated as A-CNFs@DE. In an alternative formulation, DBU was introduced alongside glycerol in equal proportions (1 : 1 ratio). The subsequent processing steps remained the same, leading to the formation of a different version of the dielectric layer, termed A-CNFs-DBU@DE.

Capacitive CO_2 sensor. A graphite ink coating was applied to a standard aluminum foil to enable the photothermal conversion of infrared light into heat. The dielectric layer comprises 3 foams of 3×3 cm^2 area each with a thickness of *ca.* 400 μm was then enclosed between two such aluminum foils. To ensure structural integrity and prevent delamination, the entire assembly was securely sealed along the edges with tape. The area of the electrode was 8×2.5 cm^2 with a thickness of 15 μm.

Characterization

Sample morphology was examined *via* scanning electron microscopy (SEM) on a JEOL JSM-7000F instrument. Elemental composition was determined through combustion analysis. Attenuated total reflectance Fourier transform infrared spectroscopy (ATR-FTIR) spectra were acquired using a Varian 610-IR FT-IR spectrometer, set at 4 cm^{-1} resolution over 32 scans. Zeta-potential measurements were conducted at 298 K using a Malvern Zetasizer Nano instrument. Thermogravimetric Analysis (TGA) was performed under an N_2 atmosphere using a TA Instruments. Discovery thermobalance, monitoring mass loss from 30 to 800 °C at a rate of 10 °C min^{-1}. N_2 sorption and CO_2 sorption isotherms were conducted on a Micromeritics ASAP2020 at 77 K and 273.15 K, respectively. Prior to these measurements, all the samples were rigorously degassed for 10 hours at 80 °C under vacuum. The Brunauer–Emmett–Teller (BET) method was used for surface area determination. The capacitance measurement was detected using a capacitance meter.

Results and discussion

The functionalization step introduces a primary amine 3-aminopropyl(diethoxy)methylsilane (APDEMS) onto the CNFs, which significantly improves their CO_2 capture capacity of CNFs through chemisorption.[24] The functionalized CNFs demonstrate a CO_2 uptake capacity of up to 3.2 mmol g^{-1} at 273.15 K, with an amine efficiency of 43.6%. This performance is outstanding compared to previously reported materials, as detailed in Table S1 (ESI†).

The capacitive CO_2 sensor stands out from existing technologies by effectively operating under ambient conditions and showing minimal humidity interference,[25] offering superior CO_2 selectivity.[26] It relies on the principle of detecting changes in the capacitance of the CNF material in response to CO_2 exposure, which alters their electrical properties.[27] This change in capacitance, quantitatively indicative of the CO_2 levels, can then be converted into a readable electrical signal. The sensor's design also integrates photothermal graphite ink-coated aluminium electrodes, potentially contributing to enhanced energy efficiency.[28] All these aforementioned features enable the sensor designed here suitable for a variety of applications, including in smart buildings,[29] environmental monitoring,[30] and industrial safety.[31] Our study, centered on the chemisorption mechanism of CO_2 by aminated cellulose nanofibrils, skips the direct selectivity tests due to the well-established specificity of the chemisorption process towards CO_2, supported by extensive literature.[32,33] Its high sensitivity and specificity render it particularly qualified for critical scenarios such as indoor air quality assessment,[34] and ventilation control,[35] largely contributing to environmental sustainability and public health.

As a starting material, commercial 2,2,6,6-tetramethyl-1-piperidinyloxy (TEMPO)-oxidized CNFs were used and functionalized with 3-aminopropyl(diethoxy)methylsilane (APDEMS) in an aqueous medium, to graft primary amine groups onto their surface, as depicted in Scheme 1.

This modification occurs through the hydrolysis of APDEMS to form reactive silanol groups,[36] which next can undergo condensation reaction either with themselves through the silanol groups (–Si–O–H) or with the hydroxyl groups present on the CNFs surface.[37] The former results in the connection of APDEMS molecules, while the latter leads to the grafting of primary amine groups onto the CNFs. Such functionalization significantly enhances the CNFs' capability for CO_2 chemisorption, primarily through the formation of carbamate species

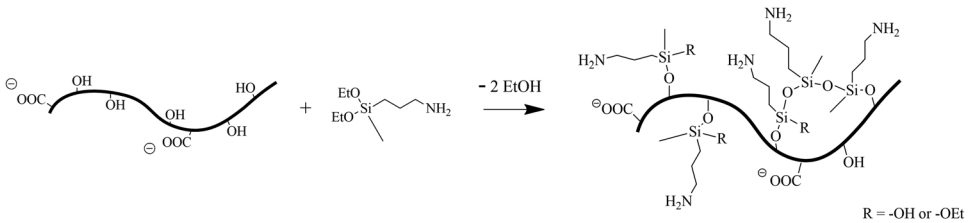

Scheme 1 Schematic of the grafting of APDEMS onto cellulose nanofibrils *via* sequential hydrolysis and condensation reactions in an aqueous environment.

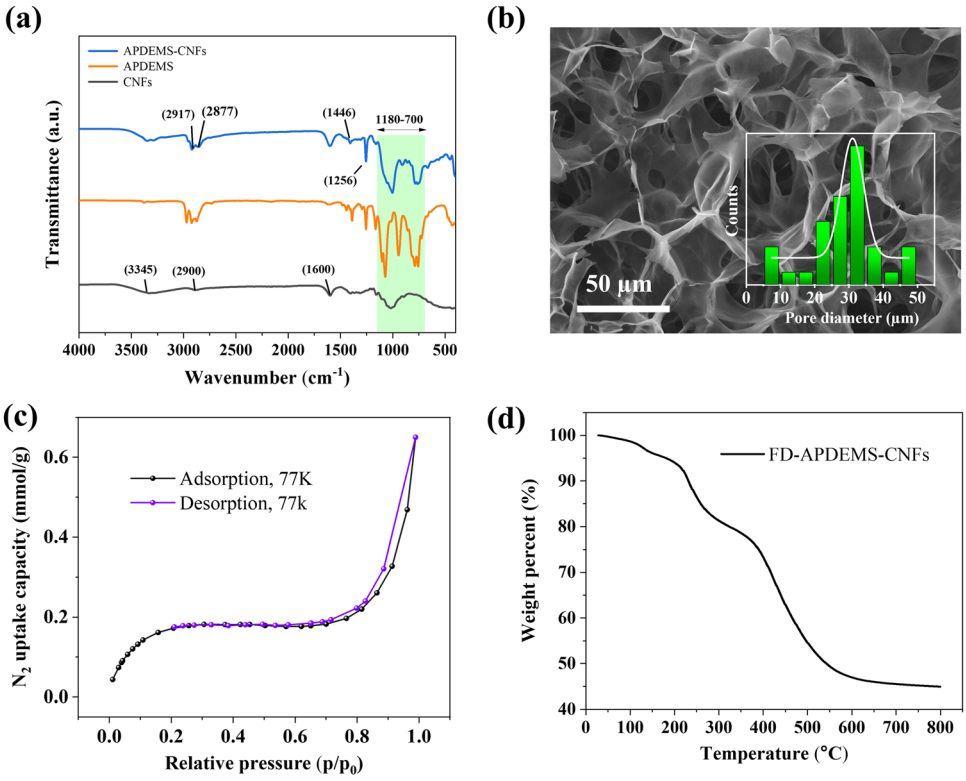

Fig. 1 (a) FTIR spectra for CNFs, APDEMS, and APDEMS-CNFs hydrogel, revealing their chemical structures and functional groups. (b) Cross-sectional SEM image of FD-APDEMS-CNFs. (c) N_2 sorption isotherm of FD-APDEMS-CNFs, depicting its adsorption–desorption behavior and pore size distribution. (d) TGA results for FD-APDEMS-CNFs, indicating its thermal stability.

or derivatives. This chemical modification is subsequently analysed through rheological studies, as presented in Fig. S1 (ESI†).

FTIR analysis, shown in Fig. 1a, supported the successful grafting of APDEMS onto CNFs. Key spectral features in APDEMS-CNFs include the –CH stretching vibrations at 2917 cm^{-1} and 2877 cm^{-1}, $–CH_2$ bending at 1446 cm^{-1}, and bands at 1256 cm^{-1} ($\nu_{Si–C}$) as well as in the 1180 to 700 cm^{-1} range, indicating –Si–O-based linkages. Additionally, characteristic cellulose bands, *e.g.*, the –OH stretching at 3345 cm^{-1}, –CH stretching at 2900 cm^{-1}, and –COO-stretching at 1600 cm^{-1} were also present, showcasing the integrity of the cellulose structure after post-functionalization. The atomic force microscopy (AFM) analysis of the CNFs prior to APDEMS functionalization revealed a homogenous nanofibril structure with an average thickness of 2.6 ± 0.5 nm (Fig. S2, ESI†). Upon amination, the produced APDEMS-CNFs show a similar morphology in AFM analysis.

Following the surface functionalization, the CNF-based reaction mixture was directly freeze-dried from their aqueous solution, forming a dried foam structure named FD-APDEMS-CNFs.

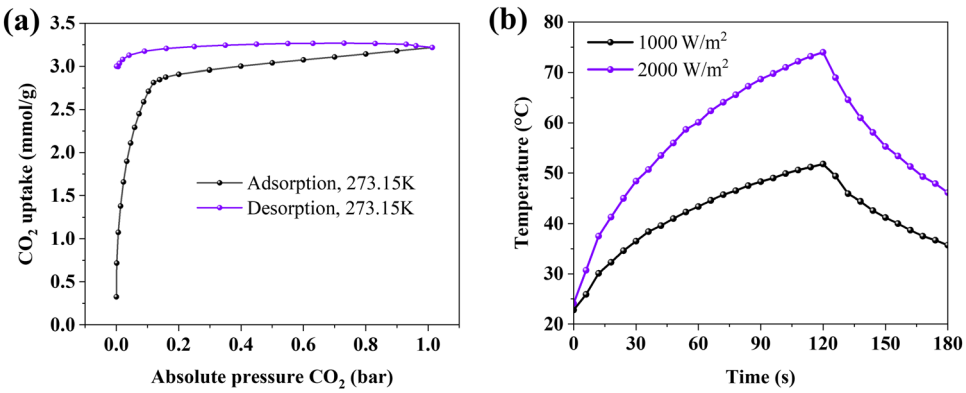

Fig. 2 (a) CO_2 sorption isotherm of FD-APDEMS-CNFs measured at 273.15 K. (b) Evaluation of the photothermal performance of graphite ink-coated aluminum foil under two IR irradiation intensities (10^3 W m^{-2} and 2 × 10^3 W m^{-2}), assessed over two minutes, followed by a one-minute temperature decrease recording.

Table 1 Comparative analysis of BET surface area, nitrogen composition, amine loading, and amine efficiency between FD-CNFs and FD-APDMS-CNFs samples

Sample	BET	%N	CO_2 uptake
FD-CNFs	29.6 ± 3.1 m^2 g^{-1}	0.00 ± 0.01	0.1 ± 0.1 mmol g^{-1}
FD-APDEMS-CNFs	17.3 ± 3.6 m^2 g^{-1}	10.29 ± 0.01	3.2 ± 0.2 mmol g^{-1}

The dry foam was characterized using scanning electron microscopy (SEM), revealing a network of interconnected pores, averaging 31.1 μm in pore diameter (Fig. 1b). Additionally, nitrogen (N_2) sorption isotherms conducted on the foam revealed a low specific surface area of 17.3 m^2 g^{-1} *via* the Brunauer–Emmett–Teller (BET) equation (Fig. 1c), showing its macroporous nature, in accordance with the SEM image analysis in Fig. 1b. Furthermore, thermogravimetric analysis (TGA) of FD-APDEMS-CNFs, shown in Fig. 1d, indicated its thermal stability up to 205 °C, with a slight decrease step in mass around 100–130 °C primarily due to desorption of chemisorbed CO_2.

The CO_2 uptake capacity of FD-APDEMS-CNFs was evaluated through comprehensive CO_2 gas sorption measurements at 273.15 K, as depicted in Fig. 2a. The isotherm demonstrates significant CO_2 sorption, achieving up to 3.2 mmol g^{-1}, and is particularly effective in the low partial pressure range below $p/p_0 < 0.1$. This enhanced sorption efficiency in the low pressure range is attributed to the chemisorption process, wherein CO_2 molecules form strong chemical bonds with the primary amine sites of the aminated CNFs. This interaction is highly efficient even at rather low CO_2 concentrations, highlighting the potential of functionalized CNFs for effective CO_2 capture in environments of diluted CO_2 steams. Such a feature makes these CNFs a promising absorber for applications in real-world ambient scenarios. The characterization of FD-APDEMS-CNFs, including elemental analysis, is detailed in Table 1, and is compared with freeze-dried pristine cellulose nanofibrils, termed FD-CNFs, which serves as the control sample.

A capacitive CO_2 sensor detects CO_2 concentrations by measuring changes in the capacitance of a sensing material. Here, this sensor comprises two graphite ink-coated aluminum foil electrodes and a CO_2-sensitive dielectric layer (DE) derived from FD-APDEMS-CNFs foams. The graphite ink coating on the electrodes enhances CO_2 desorption efficiency through photothermal conversion where infrared light (IR) can be absorbed by the graphite ink to heat the electrodes (Fig. 2b). The absorption of infrared (IR) for heating is confirmed through an additional IR test. Utilizing 1000 W m^{-2} and 2000 W m^{-2} radiation levels, varied practical heating scenarios are simulated, demonstrating the sensor's efficacy across different environmental conditions. This highlights the sensor's capacity to attain the optimal temperature for efficient CO_2 desorption. The comparative approach offers a comprehensive reference for the sensor's performance under diverse conditions.

In this work, two distinct versions of the CO_2-sensitive DE were developed: A-CNFs@DE, which serves as the reference, is a mixture of FD-APDEMS-CNFs and glycerol (mass ratio = 1 : 1), with glycerol as additive to enhance the foam plasticity; and A-CNFs-DBU@DE, which further incorporates a strong base DBU molecule (an equal mass to glycerol).

It is hypothesized that upon exposure to CO_2, the sensor's DE absorbs the gas molecules mainly though the chemisorption mechanism through the CNFs' primary amine functionality to form carbamate-based ion pairs. This process results in the immediate polarization of the DE, increasing the dielectric constant (κ) and, consequently, the sensor's capacitance (eqn (1)).

$$C = \frac{\kappa \varepsilon_0 A}{d} \tag{1}$$

The capacitance of a plate capacitor. This equation describes the capacitance of a plate capacitor, where C is the capacitance, κ the dielectric constant, ε_0 the vacuum permittivity, A the plate area, and d the plate separation.

In the A-CNFs-DBU@DE sample, DBU, a strong base, is added to play a pivotal role. Its addition is theorized to promote the formation of mobile protonated DBU cationic species. Note that the addition of glycerol to FD-APDEMS-CNFs facilitates the formation of ammonium carbamate in A-CNFs@DE, where both cation and anion are immobilized on the CNF surface;

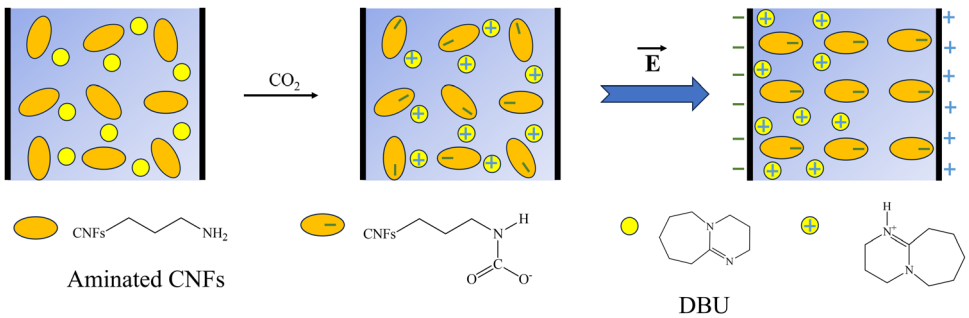

Fig. 3 Illustration depicting capacitance changes in A-CNFs-DBU@DE sensors, triggered by CO_2 exposure and further amplified by the alignment of protonated DBU cations within an electric field as well as the assumed scheme of the ions.

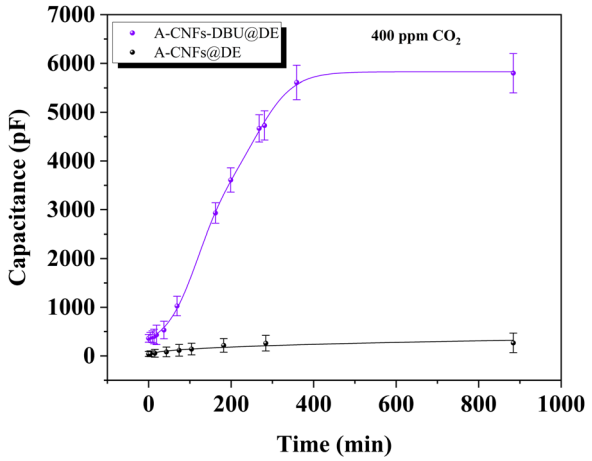

Fig. 4 Dynamic capacitance profiles of A-CNFs@DE and A-CNFs-DBU@DE CO_2 sensors under controlled conditions (400 ppm CO_2, 35% RH, and 21.0 °C). Each data in the profile is the average value obtained in three sequential sorption curves.

by the addition of DBU into A-CNFs-DBU@DE that has a higher pK_a (12.0) than the alkyl amine unit (~10.7), DBU will accept the proton to form the much mobile protonated DBU cation that is not covalently bonded to the CNF. When these species align in an electric field, they significantly enhance the sensor's capacitance by drastically increasing κ (Fig. 3), where the effect is much stronger for A-CNFs-DBU@DE due to its mobile protonated DBU cations than the A-CNFs@DE without mobile ions.

After a one-hour CO_2 desorption phase at 90 °C, we observed the capacitance changes in both sensors, A-CNFs@DE and A-CNFs-DBU@DE, under a two-hour, 400 ppm CO_2 exposure. The A-CNFs@DE sensor showed a notable increase in capacitance from 41 pF to 262 pF, by 539%, whereas the A-CNFs-DBU@DE sensor exhibited a more significant rise from 500 pF to 5600 pF, an increase by 1020%, primarily due to the integration of the protonated DBU. The as-prepared sensors exhibited the capability to recover to their initial state post CO_2 exposure in a 3-sequential CO_2 sorption-desorption cycles (Fig. 4 and Fig. S3, S4, ESI†).

Additionally, the dynamics of capacitance change (ΔC) was assessed in a pure CO_2 environment (Fig. 5a). There, A-CNFs@DE sensor showed a rapid initial response thanks to its higher CO_2 sorption capacity of 2.4 mmol g^{-1} at 1 bar CO_2, whereas the A-CNFs-DBU@DE variant, with a lower capacity of 0.55 mmol g^{-1} (Fig. 5b and Movie S1, ESI†), had a more gradual response.

Those experiments conducted in both ambient and pure CO_2 atmospheres, revealed that high CO_2 affinity by chemisorption leads to rapid initial shifts in capacitance. Over time, however, the role of mobile cations becomes increasingly significant in determining the capacitance, leading to larger and more sustained changes in capacitance.

Conclusion

The chemical functionalization of cellulose nanofibrils with APDEMS to attach primary amine groups onto CNFs surface markedly enhanced their CO_2 sorption capacity, reaching up to 3.2 mmol g^{-1}. By incorporating these aminated CNFs into the dielectric layer of a capacitive sensor, complemented by photothermal graphite ink-coated aluminum electrodes, has led to the creation of a highly sensitive CO_2 sensor. Notably, the DBU-integrated one, A-CNFs-DBU@DE, demonstrates significant capacitance increases in response to CO_2 exposure, showcasing its exceptional potential for precise CO_2 detection. Its high sensitivity renders it particularly suitable for critical CO_2 monitoring applications. Future research efforts aim to optimize the sensor design, enhancing sensitivity, reducing response times and improving long-term stability. These efforts bridge the gap between basic materials research and practical CO_2-sensing applications. The promising results of this study establish a strong foundation for advancing CO_2 sensing technology, representing a conductive step towards effective environmental monitoring.

Author contributions

Frédéric Héraly: contributed to the conceptualization of the study, investigation, data curation, and formal analysis.

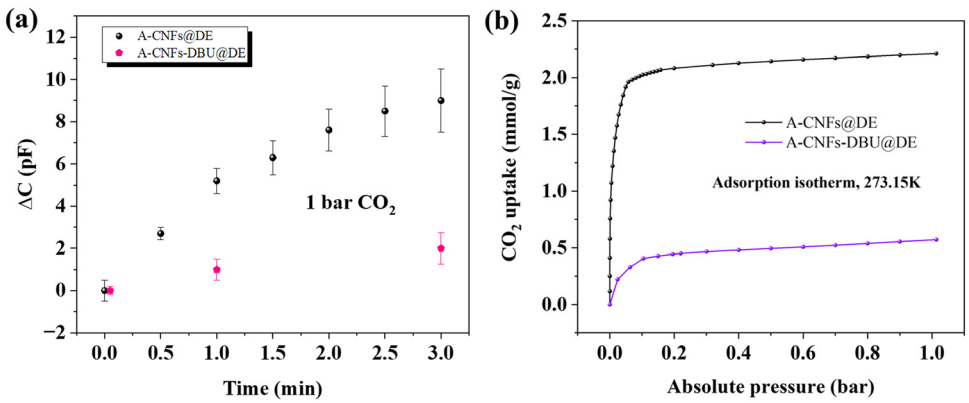

Fig. 5 (a) Comparative analysis of the capacitance change response of the two sensors within the initial 3 minutes of exposure in a 1 bar CO_2 environment at 40% RH and a temperature of 21.2 °C. (b) Evaluation of their CO_2 capture performance through gas sorption analysis, measured at 273.15 K.

Responsible for writing the original draft and involved in the review and editing process. Anirban Sikdar: participated in the final review of the manuscript. Jian Chang: participated in the final review of the manuscript. Jiayin Yuan: contributed to the conceptualization of the study, as well as investigation and formal analysis.

Conflicts of interest

There are no conflicts to declare.

Acknowledgements

This work was supported by the Wallenberg Academy Fellow program from the Knut & Alice Wallenberg Foundation (grant number KAW 2017.0166 and KAW2022.0194), and the Swedish Research Council Grant 2022-04533.

References

1 W. J. Ripple, C. Wolf, T. M. Newsome, P. Barnard and W. R. Moomaw, World scientists' warning of a climate emergency, *BioScience*, 2020, **70**, 8–100.
2 R. Tuckett, *Encyclopedia of Analytical Science*, Elsevier, 2019, pp. 362–372.
3 H. Ritchie, M. Roser and P. Rosado CO_2 and greenhouse gas emissions, *Our world in data*, (2020).
4 A. Molina, V. Escobar-Barrios and J. Oliva, A review on hybrid and flexible CO_2 gas sensors, *Synth. Met.*, 2020, **270**, 116602.
5 A. Borodinecs, A. Palcikovskis and V. Jacnevs, Indoor Air CO_2 Sensors and Possible Uncertainties of Measurements: A Review and an Example of Practical Measurements, *Energies*, 2022, **15**, 6961.
6 M. Y. Rezk, J. Sharma and M. R. Gartia, Nanomaterial-based CO_2 sensors, *Nanomaterials*, 2020, **10**, 2251.
7 A. Kumar, H. Kim and G. P. Hancke, Environmental monitoring systems: A review, *IEEE Sens. J.*, 2012, **13**, 1329–1339.
8 A. T. Guntner, *et al.*, Breath sensors for health monitoring, *ACS Sens.*, 2019, **4**, 268–280.
9 J. Wu, *et al.*, *In situ* μ-printed optical fiber-tip CO_2 sensor using a photocrosslinkable poly (ionic liquid), *Sens. Actuators, B*, 2018, **259**, 833–839.
10 G. F. Fine, L. M. Cavanagh, A. Afonja and R. Binions, Metal oxide semi-conductor gas sensors in environmental monitoring, *Sensors*, 2010, **10**, 5469–5502.
11 D. Gibson and C. MacGregor, A novel solid state non-dispersive infrared CO_2 gas sensor compatible with wireless and portable deployment, *Sensors*, 2013, **13**, 7079–7103.
12 R. K. Jha, Non-dispersive infrared gas sensing technology: A review, *IEEE Sens. J.*, 2021, **22**, 6–15.
13 Y. Zhou, Y. Wang, Y. Wang and X. Li, Humidity-enabled ionic conductive trace carbon dioxide sensing of nitrogen-doped Ti_3C_2Tx MXene/polyethyleneimine composite films decorated with reduced graphene oxide nanosheets, *Anal. Chem.*, 2020, **92**, 16033–16042.
14 Y. Zhou, *et al.*, Amine-functionalized black phosphorus nanosheets toward ultrafast and room-temperature trace carbon dioxide sensing, *J. Phys. Chem. Lett.*, 2022, **13**, 9599–9606.
15 N. Yamazoe, Toward innovations of gas sensor technology, *Sens. Actuators, B*, 2005, **108**, 2–14.
16 X. Liu, *et al.*, A survey on gas sensing technology, *Sensors*, 2012, **12**, 9635–9665.
17 T. Ishihara and S. Matsubara, Capacitive type gas sensors, *J. Electroceram.*, 1998, **2**, 215–228.
18 J. Boudaden, A. Klumpp, H.-E. Endres and I. Eisele, Towards low cost and low temperature capacitive CO_2 sensors based on amine functionalized silica nanoparticles, *Nanomaterials*, 2019, **9**, 1097.
19 R. Zhang, *et al.*, Mesoporous cellulose nanofibers-interlaced PEDOT: PSS hybrids for chemiresistive ammonia detection, *Microchim. Acta*, 2022, **189**, 308.
20 Y. Zhou, *et al.*, Alkalized Cellulose Nanofiber-Interweaved PEDOT: PSS Thin-Film Sensors via Layer-by-Layer Spraying Assembly for Ultrafast Molecular Ammonia Detection, *ACS Appl. Mater. Interfaces*, 2023, **15**, 53802–53814.
21 A. Isogai, T. Saito and H. Fukuzumi, TEMPO-oxidized cellulose nanofibers, *Nanoscale*, 2011, **3**, 71–85.
22 T. Saito, S. Kimura, Y. Nishiyama and A. Isogai, Cellulose nanofibers prepared by TEMPO-mediated oxidation of native cellulose, *Biomacromolecules*, 2007, **8**, 2485–2491.
23 T. Li, *et al.*, Developing fibrillated cellulose as a sustainable technological material, *Nature*, 2021, **590**, 47–56.
24 E. E. Ünveren, B. Ö. Monkul, Ş. Sarıoğlan, N. Karademir and E. Alper, Solid amine sorbents for CO_2 capture by chemical adsorption: A review, *Petroleum*, 2017, **3**, 37–50.
25 S. Riyazi and M. Azim Araghi, Performance of interdigitated capacitive-type CO_2 sensor based on polypyrrole/copper phthalocyanine nanocomposite, *J. Mater. Sci.: Mater. Electron.*, 2020, **31**, 3539–3548.
26 Z. Zhai, X. Zhang, X. Hao, B. Niu and C. Li, Metal–Organic Frameworks Materials for Capacitive Gas Sensors, *Adv. Mater. Technol.*, 2021, **6**, 2100127.
27 P. Bindra and A. Hazra, Capacitive gas and vapor sensors using nanomaterials, *J. Mater. Sci.: Mater. Electron.*, 2018, **29**, 6129–6148.
28 G. Liu, J. Xu and K. Wang, Solar water evaporation by black photothermal sheets, *Nano Energy*, 2017, **41**, 269–284.
29 A. H. Buckman, M. Mayfield and B. M. Beck, S. What is a smart building?, *Smart Sustainable Built Environ.*, 2014, **3**, 92–109.
30 M. Struzik, I. Garbayo, R. Pfenninger and J. L. Rupp, A simple and fast electrochemical CO_2 sensor based on $Li_7La_3Zr_2O_{12}$ for environmental monitoring, *Adv. Mater.*, 2018, **30**, 1804098.
31 S. Neethirajan, D. Jayas and S. Sadistap, Carbon dioxide (CO_2) sensors for the agri-food industry—a review, *Food Bioprocess Technol.*, 2009, **2**, 115–121.
32 C. Gebald, J. A. Wurzbacher, P. Tingaut and A. Steinfeld, Stability of amine-functionalized cellulose during temperature-vacuum-swing cycling for CO_2 capture from air, *Environ. Sci. Technol.*, 2013, **47**, 10063–10070.
33 C. Gebald, J. A. Wurzbacher, P. Tingaut, T. Zimmermann and A. Steinfeld, Amine-based nanofibrillated cellulose as

adsorbent for CO_2 capture from air, *Environ. Sci. Technol.*, 2011, **45**, 9101–9108.
34 A. Cincinelli and T. Martellini, *Indoor Air Quality and Health*, MDPI, 2017, vol. 14, p. 1286.
35 W. J. Fisk, CO2 monitoring for demand controlled ventilation in commercial buildings, (2010).
36 S. Savard, L. P. Blanchard, J. Léonard and R. Prud'Homme, Hydrolysis and condensation of silanes in aqueous solutions, *Polym. Compos.*, 1984, **5**, 242–249.
37 Y. Xie, C. A. Hill, Z. Xiao, H. Militz and C. Mai, Silane coupling agents used for natural fiber/polymer composites: A review, *Composites, Part A*, 2010, **41**, 806–819.

